2011 American Control Conference
on O'Farrell Street, San Francisco, CA, USA
June 29 - July 01, 2011

Adaptive Trajectory Tracking Control of Microcantilever's Tip used in AFM with a General Nonlinear Tip-Sample Interaction Force

Sohrab Eslami, *IEEE student member*, Nader Jalili, Darren M. Dawson

Abstract **— This paper presents an adaptive trajectory tracking control of microcantilever's tip used in AFM systems with a general nanomechanical tip-sample interaction force. This controller is capable of dealing with uncertainties such as tip mass, damping coefficients and the complicated nature of the nonlinear interaction force present in the AFM systems. For this, a distributed-parameters based model for microcantilever with a tip mass is developed. On the other hand, a general interaction force between the tip and surface of the sample is assumed here which affects the microcantilever's response and due to its intrinsic nonlinearity, it adds complexity to the system. Simulation results demonstrate that proposed adaptive controller is capable of precise trajectory tracking with various applications in manipulation of and imaging systems.**

I. Introduction

OVER the past decade, many studies focused on different measurement and imaging techniques at the micro/nano scale. One of these prominent approaches is the atomic force microscopy (AFM) with three modes; contact, tapping and non-contact. However, non-contact AFM mode has evolved into the center of attention due to its true atomic resolution [1, 2]. One of the advantages of AFM is attributed to manipulation of nanoparticles in chemical, material, electronics, pharmaceutical and medical categories with different interaction forces including van der Waals, electrostatic and capillary [3, 4 and 5]. Due to the nature of the non-contact mode, the sample is not crashed or burst; therefore, this method is considered as a non-destructive tool for handling soft biological samples or determining the properties of cells (e.g., stress-strain characteristics) to detect the cancer cells [6, 7 and 8]. Another application of AFM is recognizing the nanoparticles inside the cells which other methods are not capable of providing such resolution. More specifically, this information is provided by the scanning near field ultrasonic holography technique [9, 10] with notable advantages in drug delivery and nanotoxicology.

Nanomedicine and nanosurgery have taken advantage of precision, less damage and more surface observation of the AFM-based technique for treating the living cells to create new drugs and gene therapy compared to the other methods such as microcapillary-based apparatus regardless of the cell size [11]. Moreover, AFM has been utilized in nano-neurosurgery for imaging the interface between the neuron cells and glial or observation of the brain tumor cell invasion process [12, 13].

In order to have better understanding of AFM, it is required to model such system elaborately under the realistic conditions considering a comprehensive model to reveal the response of the system appropriately. Some studies have considered a lumped-parameters representation [14, 15] which is not accurate for higher frequencies that are encountered in higher modes of operation. On the other hand, some comprehensive beam models considering the shear deformation and rotary inertia represent the system response in more highly structured fashion [16] but are too difficult for the real-time control implementation particularly when it is desired to consider a nonlinear interaction force.

Due to existence of many uncertainties for a system in the scale of micro or nano, a need for employing a controller to be able to eliminate the indeterminacy and disturbance is arisen for some desired tasks. For this reason, appropriate control techniques such as optimal LQR law control [17] and adaptive controller [18, 19] have been recently developed to achieve a stable and fast nanomanipulation task through interacting and controlling the nanoparticles very accurately. Nonetheless, there is a feeling of necessity of related works focusing on designing an inclusive model to represent a more realistic system behavior while simultaneously presenting advanced controllers to deal with this comprehensive AFM cantilever model to control the oscillations of the probe's tip.

In this paper, a hybrid distributed-parameters model (combination of a PDE and ODE) of a microcantilever beam is exploited to represent a comprehensive model of the AFM microcantilever. There is a mechanical base excitation for this model and can be considered as an input force control to drive the microcantilever. By taking advantage of flexibility of the cantilever despite its complexity and under existence of the external nonlinear tip-sample interaction force, an adaptive controller can be applied in order to make the microcantilever's tip track a desired trajectory. This trajectory can be further considered as an important path acquired by the path planning techniques to manipulate the nanoparticles. The structure of this paper is organized as follows. Initially, the appropriate form of a distributed-parameters model of the AFM microcantilever is obtained. Secondly, an adaptive controller is developed for the

S. Eslami, PhD Candidate, Department of Mechanical and Industrial Engineering, Northeastern University, Boston, MA 02115 (e-mail: seslami@coe.neu.edu).

N. Jalili, Associate Professor and Author of Correspondence, Department of Mechanical and Industrial Engineering, Northeastern University, Boston, MA 02115 (phone: 617-373-3629; fax: 617-373-2921; e-mail: n.jalili@neu.edu).

D. M. Dawson, Professor, Holcombe Department of Electrical and Computer Engineering, Clemson University, Clemson, SC 29634 (e-mail: darren.dawson@ces.clemson.edu).

978-1-4577-0079-8/11/$26.00 ©2011 AACC

microcantilever's tip to execute the task of following a trajectory and eventually, numerical simulations are provided to show the performance and stability of the controller.

II. Problem Statement and Mathematical Modeling

In non-contact AFM and in order to sense the presence of the van der Waals forces, it is required that the base of the cantilever to be excited over the sample. Figure 1 shows a schematic of a microcantilever with a probe scanning a sample's surface under existence of the van der Waals interaction forces. The deflection of the microcantilever is determined by analyzing the laser beam reflection captured by a photodetector. This signal transmitted into the photo detector carrying the information of the tip deflection is compared with the reference and creates an error signal to enter the controller unit which further determines the required voltage to be sent out to the PZT positioner. In a recent publication by the researchers at the Oak Ridge National Laboratory [9], an AFM system collects the information inside a cell besides its conventional task for the surface imaging. In this approach, the cantilever is oscillated at a resonant frequency and a living cell mounted on a piezoelectric positioner is vibrated at a frequency close to the cantilever's resonant frequency such that an ultrasonic wave resulting from the sample excitation may interfere with the cantilever oscillation [9]. For this purpose, a distributed-parameters model of the microcantilever beam is studied here.

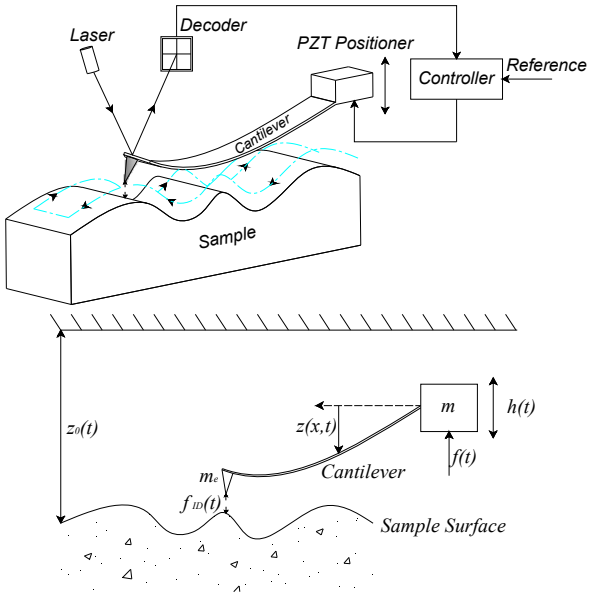

Fig. 1. A schematic of a non-contact AFM operation and modeling.

Considering the flexibility of a cantilever beam and the effects of the distributed mass along the beam, the governing hybrid equation (including PDE and ODE) of a cantilever with a base excitation can be shown as [20, 21]:

$$\rho(\ddot{z}(x,t)+\ddot{h}(t))+B\dot{z}(x,t)+C\dot{z}'(x,t)+EIz''''(x,t)=-EI\times g''''(x)f_{ID}(t)-Bg(x)\dot{f}_{ID}(t)-Cg'(x)\dot{f}_{ID}(t)-\rho g(x)\ddot{f}_{ID}(t) \quad (1)$$

$$(m+\rho L+m_e)\ddot{h}(t)+\int_0^L \rho\ddot{z}(x,t)dx+m_e\ddot{z}(L,t)= f(t)+f_{ID}(t)-\ddot{f}_{ID}(t)\int_0^L \rho g(x)dx \quad (2)$$

where EI is the microcantilever rigidity, ρ is the microcantilever linear density, L is the microcantilever length, m is the base mass, m_e is the tip mass, B is the microcantilever viscous damping, C is the microcantilever structural damping, $g(x)$ is a geometrical function [21], $f(t)$ is the input force to the base, $f_{ID}(t)$ is the interaction force, $h(t)$ is the base motion and $z(x,t)\in\Re^1$ is the microcantilever transverse displacement.

Homogeneous boundary conditions are as follows:

$$z(0,t)=z'(0,t)=z''(L,t)=0$$
$$m_e[\ddot{h}(t)+\ddot{z}(L,t)]=EIz'''(L,t) \quad (3)$$

In Eqs. (1-3), the superscripts $\dot{(.)}$ and $(.)'$ represent the partial derivative with respect to time and displacement, respectively.

Substituting term $\rho\ddot{h}(t)$ from Eq. (1) into Eq. (2) and performing some algebraic manipulations and simplifications, it yields:

$$\rho\ddot{z}(x,t)-(\frac{m+m_e}{L})\ddot{h}(t)-\int_0^L\frac{\rho}{L}\ddot{z}(x,t)dx-\frac{m_e}{L}\ddot{z}(L,t)+B\dot{z}(x,t)+C\dot{z}'(x,t)+EIz''''(x,t)=-\frac{f(t)}{L}-(\frac{1}{L}+EIg''''(x))f_{ID}(t)-(Bg(x)+Cg'(x))\dot{f}_{ID}(t)+(\frac{1}{L}\int_0^L\rho g(x)dx-\rho g(x))\ddot{f}_{ID}(t) \quad (4)$$

It is observed that all terms such as base excitation, input force, interaction force and its first and second order derivatives are all present in Eq. (4). Hence, this form is preferable for designing a controller. Since there is an integral expression of $\ddot{z}(x,t)$ in Eq. (4), it is challenging to design a controller based on $z(x,t)$. However, in this paper, when an AFM is run at lower frequencies such that only the fundamental mode is excited, a controller is designed to direct the applied force to the base in order to make the tip track a desired trajectory. This is the first step in designing an advanced controller for a complicated model to deal with uncertainties.

By utilizing the assumed mode model (AMM), as a combination of linear admissible functions, $\varphi_i(x)$, the solution of a free vibration problem for $z(x,t)$ can be estimated as:

$$z(x,t)=\sum_{i=1}^{\infty}\phi_i(x)q_i(t) \tag{5}$$

For the case where the system is vibrated at lower frequencies, the assumption of the first mode can be proper since the higher modes may not be included in the response. Alternatively, the controller design with term $\int_0^L \frac{\rho}{L} z_{tt}(x,t)dx$ in Eq. (4) is challenging to deal with. Therefore, Eq. (4) is rewritten in the form of:

$$\begin{aligned}&-(\frac{m+m_e}{L})\ddot{h}(t)+(\rho\varphi_i(x)-\int_0^L\frac{\rho}{L}\varphi_i(x)dx-\frac{m_e}{L}\varphi(L))\ddot{q}(t)\\&+(B\varphi_i(x)+C\varphi_i'(x))\dot{q}(t)+EI\varphi_i''''(x)q(t)=-\frac{f(t)}{L}-\\&(\frac{1}{L}+EIg''''(x))f_{ID}(t)-(Bg(x)+Cg'(x))\dot{f}_{ID}(t)+\\&(\frac{1}{L}\int_0^L\rho g(x)dx-\rho g(x))\ddot{f}_{ID}(t)\end{aligned} \tag{6}$$

After pre-multiplying both sides of Eq. (6) by $\varphi_j(x)$ and integrating from 0 to L and executing some simplifications, the following expression can be obtained:

$$\begin{aligned}&\left\{\int_0^L\rho\varphi_i^2(x)dx-\int_0^L\varphi_i(x)\int_0^L\frac{\rho}{L}\varphi_i(y)dydx-\int_0^L\frac{m_e}{L}\varphi_i(x)\varphi_i(L)dx\right\}\ddot{q}(t)\\&-\ddot{h}(t)\int_0^L(\frac{m+m_e}{L})\varphi_i(x)dx+\left\{B\int_0^L\varphi_i(x)\varphi_j(x)dx+C\int_0^L\varphi_i(x)\varphi_j'(x)dx\right\}\dot{q}(t)\\&+m_e\varphi_i(L)\ddot{h}(t)+m_e\varphi_i^2(L)\ddot{q}(t)+q(t)\int_0^L EI\varphi_i''^2(x)dx=-f(t)\int_0^L\frac{1}{L}\varphi_i(x)dx\\&-f_{ID}(t)\int_0^L(\frac{1}{L}+EIg''''(x))\varphi_i(x)dx-\dot{f}_{ID}(t)\int_0^L(Bg(x)+Cg'(x))\varphi_i(x)\\&-\ddot{f}_{ID}(t)(\int_0^L\rho g(x)\varphi_i(x)dx-\frac{1}{L}\int_0^L\varphi_i(x)\int_0^L\rho g(y)dydx)\end{aligned} \tag{7}$$

where term $m_e\varphi_i(L)\ddot{h}(t)+m_e\varphi_i^2(L)\ddot{q}(t)+q(t)\int_0^L EI\varphi_i''^2(x)dx$ and boundary condition (3) are replaced with $q(t)\int_0^L EI\varphi_i(x)\varphi''''(x)$. As seen, there is a term $f(t)$ in Eq. (7) which can be utilized as the control input to the base of the microcantilever in order to control the AFM probe's tip as will be discussed in the next section.

The compact form of Eq. (7) can be represented by:

$$\begin{aligned}&A_i\ddot{h}(t)+N_i\ddot{q}_i(t)+\sum_{j=1}^{i}\bar{C}_{ij}\dot{q}_j(t)+S_iq_i(t)=D_{1i}f(t)+\\&D_{2i}f_{ID}(t)+D_{3i}\dot{f}_{ID}(t)+D_{4i}\ddot{f}_{ID}(t),\quad i=1\end{aligned} \tag{8}$$

where the coefficients in Eq. (8) may be defined as:

$$\begin{aligned}&N_i=\rho\int_0^L\varphi^2{}_i(x)dx-\int_0^L\varphi_i(x)\int_0^L\frac{\rho}{L}\varphi_i(y)dy\,dx-\\&\int_0^L\frac{m_e}{L}\varphi_i(x)\varphi_i(L)dx+m_e\varphi_i^2(L)\\&A_i=-\int_0^L(\frac{m+m_e}{L})\varphi_i(x)dx+m_e\varphi_i(L)\\&\bar{C}_{ij}=\int_0^L\varphi_i(x)\left[B\varphi_j(x)+C\varphi_j(x)\right]dx\\&S_i=EI\int_0^L\varphi_i''^2(x)dx\\&D_{1i}=-\int_0^L(\frac{1}{L}+EIg''''(x))\varphi_i(x)dx\\&D_{2i}=-\int_0^L(Bg(x)+Cg'(x))\varphi_i(x)dx\\&D_{3i}=-\int_0^L\rho g(x)\varphi_i(x)dx+\frac{1}{L}\int_0^L\varphi_i(x)\int_0^L\rho g(y)dy\,dx\\&D_{4i}=-\frac{1}{L}\int_0^L\varphi_i(x)dx\end{aligned} \tag{9}$$

In deriving Eq. (8), the following orthogonality conditions are implemented.

$$\begin{aligned}&\rho\int_0^L\varphi_i(x)\varphi_j(x)dx+m_e\varphi_i(L)\varphi_j(L)=N_i\delta_{ij}\\&EI\int_0^L\varphi_i''(x)\varphi_j''(x)dx=S_i\delta_{ij}\end{aligned} \tag{10}$$

In the previous work of the authors [22], a general model for the interaction force has been proposed as:

$$\begin{aligned}f_{ID}(t)=&\frac{H_1}{(z_0(t)-(\sum_{i=1}^{\infty}\varphi_i(x)q_i(t)+h(t)))^2}-\\&\frac{H_2}{(z_0(t)-(\sum_{i=1}^{\infty}\varphi_i(x)q_i(t)+h(t)))^8}\end{aligned} \tag{11}$$

where the sample topography (e.g., $h_s(t)$) is included in $z_0(t)$ for $z_0(t)>R>0$ (R is a constant positive value) and the first and second time derivatives of the interaction force can be obtained accordingly [22].

III. Adaptive Trajectory Tracking Control Development

In this section, it is attempted to develop a trajectory tracking controller for the microcantilever's tip in the presence of nonlinear tip-sample interaction forces. Therefore, an adaptive tracking controller analysis is performed to acquire this requirement in this section. As mentioned earlier, this work is the first step concentrating on the control development only for the first mode when the system is excited at lower frequencies (i.e., $z(x,t)=\sum_{i=1}^{n}\varphi_i(x)q_i(t), i=1$). If $q_d(t)\in \mathrm{R}^1$ is the desired tip displacement trajectory, an error signal may be defined as follows:

$$e(t)=q_d(t)-q_i(t)\equiv q_d(t)-q(t) \tag{12}$$

The filtered tracking error variable denoted by $r(t) \in \mathrm{R}^n$ is [23]:

$$r(t) = \dot{e}(t) + \alpha e(t) \tag{13}$$

after taking the time derivative once and substituting for $\ddot{e}(t),\ \dot{e}(t)$, it gives:

$$\dot{r}(t) = (\ddot{q}_d(t) - \ddot{q}(t)) + \alpha(\dot{q}_d(t) - \dot{q}(t)) \tag{14}$$

Pre-multiplying both sides of Eq. (14) by $M(q)$, multiplying Eq. (8) by γ and substituting for $\ddot{q}(t)$ from Eq. (8) into Eq. (14) and using Eq. (11) and its higher time derivatives, it yields:

$$M(q)\dot{r} = Y\theta - D_1\gamma u - \frac{\dot{M}}{2}r \tag{15}$$

where $Y\theta$ can be defined as follows with the assumption that $h(t) = \varphi_1(0)q_1(t)$:

$$\begin{aligned} Y\theta = {} & M\ddot{q}_d(t) + \bar{C}\gamma\dot{q}(t) + S\gamma q(t) + A\ddot{h}(t) - 30D_2H_1(z_0(t) - \\ & (\varphi(L) + \varphi(0))q(t))^8 + D_2H_2(z_0(t) - (\varphi(L) + \varphi(0))q(t))^2 + \\ & 60D_3H_1(\dot{z}_0(t) - (\varphi(L) + \varphi(0))\dot{q}(t))(z_0(t) - (\varphi(L) + \varphi(0))q(t))^7 - \\ & 8D_3H_2(\dot{z}_0(t) - (\varphi(L) + \varphi(0))\dot{q}(t))(z_0(t) - (\varphi(L) + \varphi(0))q(t)) + \\ & 60D_4H_1\ddot{z}_0(t)(z_0(t) - (\varphi(L) + \varphi(0))q(t))^7 - \\ & 60D_4H_1\ddot{h}(t)(z_0(t) - (\varphi(L) + \varphi(0))q(t))^7 - \\ & 180D_4H_1(\dot{z}_0(t) - (\varphi(L) + \varphi(0))\dot{q}(t))^2(z_0(t) - (\varphi(L) + \varphi(0))q(t))^6 - \\ & 8D_4H_2\ddot{z}_0(t)(z_0(t) - (\varphi(L) + \varphi(0))q(t)) + \\ & 8D_4H_2\ddot{h}(t)(z_0(t) - (\varphi(L) + \varphi(0))q(t)) + \\ & 72D_4H_2(\dot{z}_0(t) - (\varphi(L) + \varphi(0))\dot{q}(t))^2 + M\alpha(\dot{q}_d(t) - \dot{q}(t)) + \frac{\dot{M}}{2}r \end{aligned} \tag{16}$$

with quantities $A, S, \bar{C}, D_1, D_2, D_3$ and D_4 being the coefficients introduced in (9) for single mode consideration, $Y(q,\dot{q}) \in \mathrm{R}^{1\times n}$ being a measurable regression vector depending on the displacement and velocity of the probe's tip and $\theta \in \mathrm{R}^{n\times 1}$ being a constant system parameter vector including the unknown parameters of the system.

Multiplying Eq. (8) by γ and substituting for $f_{ID}, \dot{f}_{ID}$ and $\ddot{f}_{ID}$, and then after collecting all coefficients for $\ddot{q}(t)$, term M can be defined as bellow:

$$\begin{aligned} M = {} & N\gamma + A\varphi(0) - D_4\Big[60H_1\varphi(L)(z_0(t) - (\varphi(L) + \varphi(0))q(t))^7 \\ & -8H_2\varphi(L)\big[z_0(t) - (\varphi(L) + \varphi(0))q(t))\big]\Big] \end{aligned} \tag{17}$$

where

$$\begin{aligned} & \gamma(q) = 30(z_0(t) - (\varphi(L) + \varphi(0))q(t))^{10} = \\ & Y_1\theta_1 = a_{10}q^{10} + a_9q^9 + a_8q^8 + a_7q^7 + a_6q^6 + \\ & a_5q^5 + a_4q^4 + a_3q^3 + a_2q^2 + a_1q^1 + a_0 \end{aligned} \tag{18}$$

in other form:

$$\gamma(q) = 30\lambda(q(t))^{10} \tag{19}$$

where $\lambda(q) = (z_0(t) - (\varphi(L) + \varphi(0))q(t))$ and there is a condition on the auxiliary function $\gamma(q) \geq R^{10} > 0$.

According to Eq. (15) and substituting for $Y\theta$ from Eq. (16) the control force input $u(t)$ can be designed as:

$$u(t) = \frac{kr}{D_4} + \frac{Y\hat{\theta}}{D_4Y_1\hat{\theta}_1} \tag{20}$$

where k is a positive constant control gain and $\hat{\theta} \in \mathrm{R}^{n\times 1}$, $\hat{\theta}_1 \in \mathrm{R}^{m\times 1}$ denote dynamic parameter estimate vectors for θ and θ_1, respectively and are produced by the following gradient control law:

$$\dot{\hat{\theta}} = \Gamma Y^T(q,\dot{q})r \tag{21}$$

$\Gamma \in \mathrm{R}^{n\times n}$ is a constant positive-definite diagonal gain matrix and

$$\dot{\hat{\theta}}_1 = proj(\mu_1) = \begin{cases} \mu_1 & \text{if } \hat{\theta}_1 \in \mathrm{int}(\Lambda) \\ \mu_1 & \text{if } \hat{\theta}_1 \in \partial(\Lambda) \text{ and } \mu_1^T\hat{\theta}_1^{\perp} \leq 0 \\ P_r^t(\mu_1) & \text{if } \hat{\theta}_1 \in \partial(\Lambda) \text{ and } \mu_1^T\hat{\theta}_1^{\perp} > 0 \end{cases} \tag{22}$$

$$\text{for } \mu = -\Gamma_1 Y_1^T(q)\frac{Y(q,\dot{q})\hat{\theta}r}{Y_1(q)\hat{\theta}_1} \text{ and } \hat{\theta}_1(0) \in \mathrm{int}(\Lambda)$$

where Λ is a convex region defined as:

$$\Lambda = \{\hat{\theta}_1 : Y_1(q,\dot{q})\hat{\theta}_1 \geq R^{10}\} \tag{23}$$

with $\mathrm{int}(\Lambda)$ and $\partial(\Lambda)$ expressed as the interior of the convex region Λ and the boundary of the region, correspondingly. $\hat{\theta}_1^{\perp}(t)$ represents a unit vector which is normal to $\partial(\Lambda)$ at the point of intersection of the boundary surface $\partial(\Lambda)$ and $\hat{\theta}_1(t)$ such that the positive direction for $\hat{\theta}_1^{\perp}(t)$ is determined as pointing away from $\mathrm{int}(\Lambda)$ ($\hat{\theta}_1^{\perp}(t)$ is only defined for $\hat{\theta}_1(t) \in \partial(\Lambda)$). $P_r^t(T)$ is the component of the vector $\mu \in \mathrm{R}^{m\times 1}$ which is tangent to $\partial(\Lambda)$ at the point of intersection of the boundary surface $\partial(\Lambda)$ and the vector $\hat{\theta}_1(t)$ [24].

IV. Stability Analysis

Theorem 1. The controller (20), (21) and (22) designed in the previous section guarantees that the tracking error and the filtered tracking error approach to zero for the global asymptotic displacement tracking in spite of all system parametric uncertainties (i.e., $\lim_{t\to\infty} e(t), r(t) = 0$).

Proof. Let's define a non-negative Lyapunov candidate $V(t) : D \to \mathrm{R}$ to be a continuously differentiable function as:

$$V(t) = \frac{1}{2}Mr^2 + \frac{1}{2}\tilde{\theta}^T\Gamma^{-1}\tilde{\theta} + \frac{1}{2}\tilde{\theta}_1^T\Gamma^{-1}\tilde{\theta}_1 \tag{24}$$

By taking the time derivative of $V(t)$ and utilizing relations (15), (16), (21) and (22), after simplifications, the following inequality can be obtained for $\dot{V}(t)$:

$$\begin{aligned}\dot{V}(t) &\le \frac{1}{2}\dot{M}r^2 + Mr\dot{r} + \tilde{\theta}^T\Gamma^{-1}\dot{\tilde{\theta}} + \tilde{\theta}_1^T\Gamma^{-1}\dot{\tilde{\theta}}_1 \\ &\le \frac{1}{2}\dot{M}r^2 + r(M\dot{r}) - \tilde{\theta}^T\Gamma^{-1}\dot{\hat{\theta}} - \tilde{\theta}_1^T\Gamma^{-1}\dot{\hat{\theta}}_1\end{aligned} \tag{25}$$

where

$$\begin{aligned}&\tilde{\theta}(t) = \theta - \hat{\theta}(t) \quad \Rightarrow \quad \dot{\tilde{\theta}}(t) = -\dot{\hat{\theta}}(t) \\ &\tilde{\theta}_1(t) = \theta_1 - \hat{\theta}_1(t) \quad \Rightarrow \quad \dot{\tilde{\theta}}_1(t) = -\dot{\hat{\theta}}_1(t)\end{aligned} \tag{26}$$

then,

$$\begin{aligned}\dot{V}(t) \le{}& \frac{1}{2}\dot{M}r^2 + r[Y\tilde{\theta} - D_4\gamma u - \frac{\dot{M}}{2}r] - \tilde{\theta}^T\Gamma^{-1}\times \\ &[\Gamma Y^T(q,\dot{q})r] - \tilde{\theta}_1^T\Gamma^{-1}[proj(-\Gamma_1 Y_1^T(q)\frac{Y(q,\dot{q})\hat{\theta}}{Y_1(q)\hat{\theta}_1}r)]\end{aligned} \tag{27}$$

Executing some algebraic manipulations and simplifications the following expression can be achieved:

$$\dot{V}(t) \le -k\gamma(q)r^T r \tag{28}$$

Therefore, exploiting (24) and (27) for a positive semi-positive $V(t)$ and a negative semi-definite $\dot{V}(t)$, it can be concluded that $V(t) \in L_\infty$. Hence, $r(t) \in L_\infty$ accordingly $e(t), \dot{e}(t), q(t), \dot{q}(t) \in L_\infty$, $\tilde{\theta}(t) \in L_\infty^n$ and $\tilde{\theta}_1(t) \in L_\infty^m$ resulting in $\hat{\theta}(t) \in L_\infty^n$ and $\hat{\theta}_1(t) \in L_\infty^n$ for the estimation of unknown parameters. Exploiting $q(t) \in L_\infty$ and the previous facts, it yields that the filtered tracking error (i.e., $\dot{r}(t)$) is also bounded. From Eq. (28) and the boundedness properties for signals $r(t) \in L_\infty, L_2$ and $\dot{r}(t)$, and Barbalat's Lemma [25] it can be concluded that:

$$\lim_{t\to\infty} r(t) = 0 \tag{29}$$

Remark 1. The interaction force proposed in Eq. (11) could approach to the actual force asymptotically if all the estimated parameters converge to the accurate values of the parameters. It can be shown that the convergence of parameters holds provided that if the regression matrix satisfies certain persistency of excitation condition [25].

V. Adaptive Controller Simulations

By taking into account the sample surface topography which is also taken as a harmonic oscillation here with the frequency close to the base motion, the displacement of the microcantilever's tip is shown in Fig. 2 (a) assuming a frequency 955 (*Hz*) for the desired trajectory with harmonic oscillation. By applying the designed adaptive tracking controller after some time the tip displacement will converge to the desired predefined trajectory. This desired trajectory may be exploited to identify the interaction forces. Figure 2 (b) and (c) demonstrate the velocity and acceleration of the microcantilever's tip with an imposed excitation on the base and under existence of the probe and sample interaction. The tracking filter error and error are depicted in Fig. 3 (a) and (b) to illustrate the magnitude of the error by passing time. However, it can be concluded that the system is approaching the desired trajectory such that the error becomes smaller and smaller. The control force as the input signal to the AFM system (i.e., $u(t)$) for values $k = 0.21$ and $\alpha = 8000$ is shown in Fig. 3 (c).

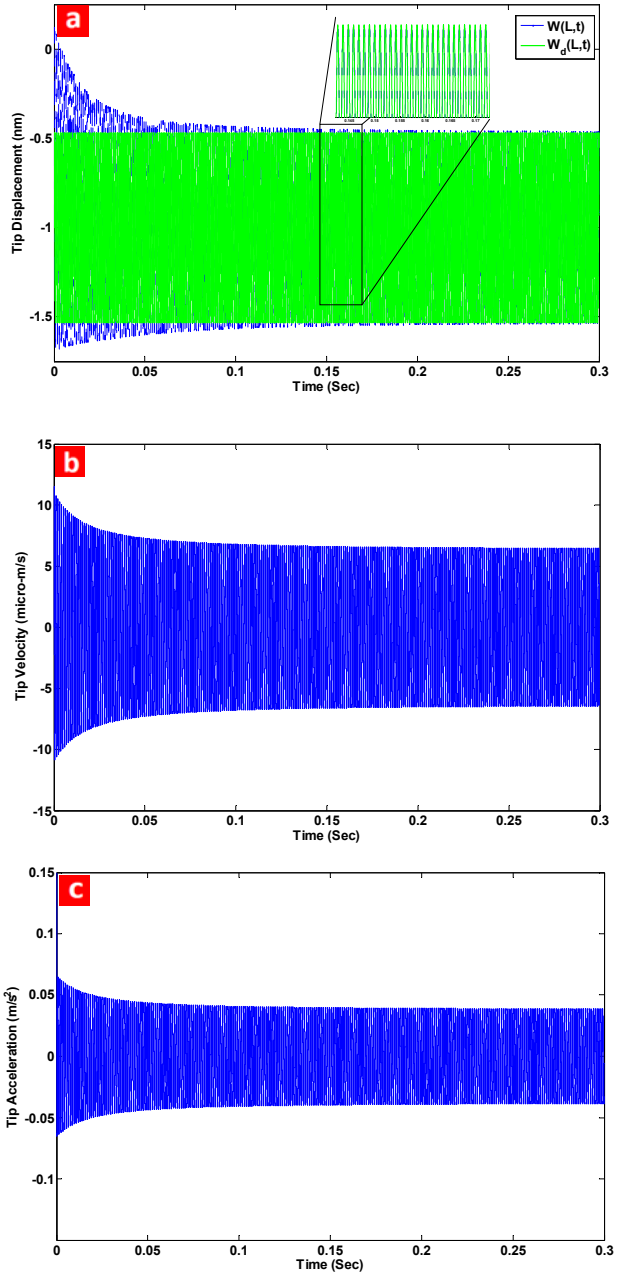

Fig. 2. a) Time history of microcantilever's tip displacement with magnification, b) velocity and c) acceleration.

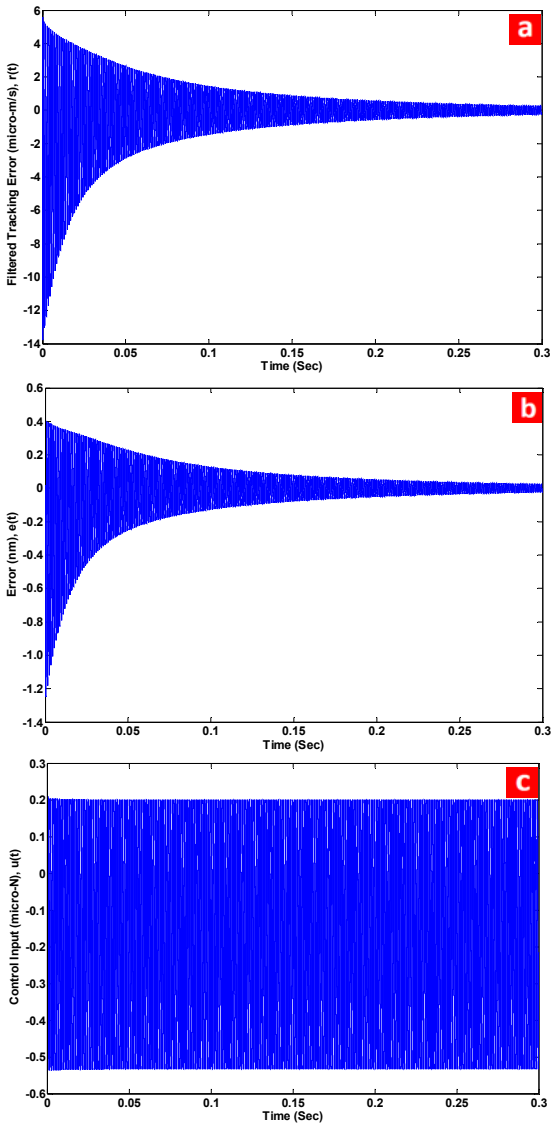

Fig. 3. a) Filtered tracking error, b) error and c) control input.

VI. Conclusions

Due to the inherent uncertainties present in AFM systems, microcantilever tip's control problems of such systems are of interest. In this paper, by taking advantage of the distributed-parameters model, the hybrid equation of the AFM was developed for the purpose of the tracking control and manipulation. A general nonlinear tip-sample interaction force was assumed for the AFM based on the tip-sample distance. Afterwards, an adaptive tracking controller was designed to asymptotically control the microcantilever's tip and simultaneously track a desired trajectory. For oscillations close to the fundamental frequency, simulation results showed the effectiveness of the proposed controller.

References

[1] R. Garcia, R. Perez, Dynamic Atomic Force Microscopy Methods, *Surface Science Reports*, **47**, pp. 197-301, 2002.

[2] N. Jalili, K. Laxminarayana, A Review of Atomic Force Microscopy Imaging Systems: Application to Molecular Metrology and Biological Sciences. *Mechatronics*, **14**, pp. 907-945, 2004.

[3] T. R. Ramachandran, C. Baur, A. Bugacov, A. Madhukar, B. E. Koel, A. Requicha and C. Gazen, Direct and Controlled Manipulation of Nanometer-Sized Particles Using the Non-Contact Atomic Force Microscope, *Nanotech.*, **9**, pp. 237-245, 1998.

[4] W. Ding, Micro/Nano-particle Manipulation and Adhesion Studies, *Adhesion Science and Tech.*, **22**, pp. 457-480, 2008.

[5] B. L. Allen, P. D. Kichambare, and A. Star, Synthesis, Characterization, and Manipulation of Nitrogen-Doped Carbon Nanotube Cups, *ACSNano*, **2** (9), pp. 1914-1920, 2008.

[6] I. Sokolov, AFM in Cancer Cell Res., in Cancer Nanotech.-Nanomater. for Cancer Diag. and Therapy (H.S. Nalwa, T. Webster), Ch 1, American Sci. Pub., Valencia, CA, ISBN 1-58883-071-3, 2006.

[7] K. Tomankova, H. Kolarova1, M. Vujtek, and H. Zapletalova, Study of Cancer Cells Used AFM, in A Méndez-Vilas, and J. Díaz (Eds.) Modern Research and Educational Topics in Microscopy, ©FORMATEX 2007.

[8] S. E. Cross, Y. S. Jin, J. Tondre, R. Wong, J. Y. Rao, and J. K. Gimzewski, AFM-Based Analysis of Human Metastatic Cancer Cells, *Nanotech.*, **19**, 384003 (8pp), 2008.

[9] L. Tetard, A. Passian, K.T. Venmar, R.M. Lynch, B.H. Voy, G. Shekawat, V.P. Dravid, T. Thundat, Imaging Nanoparticles in Cells by Nanomechanical Holography, *Nature Nanotech,* **3**, p. 501-5, 2008.

[10] G. Shekhawat, V.P. Dravid, Nanoscale Imag of Buried Struct. via Scann. Near-Field Ultrasound Holog, S*cience*, **310**, pp. 89-92, 2005.

[11] Obataya, C. Nakamura, S. W. Han, N. Nakamura, and J. Miyake, Nanoscale Operation of a Living Cell Using an Atomic Force Microscope with a Nanoneedle, *Nano Letters*, **5** (1), pp. 27-30, 2005.

[12] V. Parpura, P. G. Haydon, and E. Henderson, Three-Dimensional Imaging of Living Neurons and Glia with the Atomic Force Microscope, *Cell Science*, **104**, pp. 427-432, 1993.

[13] H. L. Fillmore, I. Chasiotis, S.W. Cho, and G. T. Gillies, AFM Observ. of Tumour Cell Invadopodia: Novel Cellular Nanomorph. on Collagen Cubstrates, *Nanotech.*, **14**, pp. 73-76, 2003.

[14] M. Ashhab, M. V. Salapaka, M. Dahleh, I. Mezic, Melnikov-Based Dynamical Analysis of Microcantilever in SPM, 1999, *Nonlinear Dynamics*, **20**, pp. 197-220, 1999.

[15] M. Basso, L. Giarre, M. Dahleh, I., Mezic, Numerical Analysis of Complex Dynamics in AFM, IEEE International Conference on Control Applications, Trieste, Italy, 1-4 Sep., pp. 1026-1030, 1998.

[16] J. C. Hsu, H. L. Lee, and W. J. Chang, Flex. Vib. Freq. of AFM Cant. Using the Timoshenko Beam Model, *Nanotech*, **18**, 285503, 2007.

[17] J. Zhang, N. Xi, G. Li, H. Y. Chan, and U. C. Wejinya, Adaptable End Effector for Atomic Force Microscopy Based Nanomanip., *IEEE Trans. on Nanotech.*, **5** (6), pp. 628-642, 2006.

[18] K. E. Rifai, O. E. Rifai, and K. Youcef-Toumi, Modeling and Control of AFM-Based Nano-Manipulation Systems, Int. Conf. on Robotics and Automation, pp. 157-162, April, Barcelona, Spain, 2005.

[19] O. M. El Rifai, K. Youcef-Toumi, On Automating AFM: An Adap. Cont. App., *Control Engineering Practice*, **15**, pp. 349-361, 2007.

[20] Y. Fang, M. Feemster , D. Dawson, N. Jalili, Active Interaction Force Identification for Atomic Force Microscope Applications, Proc. of 41st IEEE Conf. on Decision & Control, Las Vegas, NV, 2002.

[21] N. Jalili, M. Dadfarnia, D. Dawson. A Fresh Insight into the Microcantilever-Sample Interaction Problem in NC AFM, *Dynamic Systems, Measurements and Control*, **126**, pp. 327-335, 2004.

[22] S. Eslami, N. Jalili, A. Passian, L. Tetard, T. Thundat, Dynamic Nanomechanical Force Study in Microcantilevers utilized in NC AFM with App. in Nano-Scale Subsurface Imaging, to be submitted, 2011.

[23] Y. Fang, M. G. Feemster, Darren M. Dawson, N. Jalili, Nonlinear Control Techniques for the AFM System, Proc. of the 2002 ASME/IMECE, 17-22 Nov., New Orleans, LA.

[24] W. E. Dixon, A. Behal, D. M. Dawson, S. P. Nagarkatti, Nonlinear Control of Engineering Systems – A Lyapunov-Based Approach, Control Engineering (Birkhäuser) Boston, MA, 2003.

[25] J.J. Slotine, W. Li, Applied Nonlinear Control, Prentice Hall Co., Englewood Cliffs, NJ, 1991.